arXiv:quant-ph/0207047v1 9 Jul 2002

Generation of Pulsed Polarization Entangled Two-Photon State via Temporal and Spectral Engineering

Yoon-Ho Kim* and Warren P. Grice
Center for Engineering Science Advanced Research
Computer Science and Mathematics Division
Oak Ridge National Laboratory
Oak Ridge, Tennessee 37831, U.S.A.
Tel:865-241-0912; Fax:865-241-0381
(To appear in Journal of Modern Optics)

The quantum state of the photon pair generated from type-II spontaneous parametric down-conversion pumped by a ultrafast laser pulse exhibits strong decoherence in its polarization entanglement, an effect which can be attributed to the clock effect of the pump pulse or, equivalently, to distinguishing spectral information in the two-photon state. Here, we propose novel temporal and spectral engineering techniques to eliminate these detrimental decoherence effects. The temporal engineering of the two-photon wavefunction results in a universal Bell-state synthesizer that is independent of the choice of pump source, crystal parameters, wavelengths of the interacting photons, and the bandwidth of the spectral filter. In the spectral engineering technique, the distinguishing spectral features of the two-photon state are eliminated through modifications to the two-photon source. In addition, spectral engineering also provides a means for the generation of polarization-entangled states with novel spectral characteristics: the frequency-correlated state and the frequency-uncorrelated state.

I. INTRODUCTION

Quantum entanglement [1], once discussed only in the context of the foundations of quantum mechanics, is now at the heart of the rapidly developing field of quantum information science [2]. Many researchers are hoping to exploit the unique features of the entangled states in order to surpass the "classical limit" in applications such as quantum lithography [3], the quantum optical gyroscope [4], quantum clock synchronization and positioning [5], etc.

A particularly convenient and reliable source of entangled particles is the process of type-II spontaneous parametric down-conversion (SPDC) [6, 7, 8, 9, 10], in which an incident pump photon is split into two orthogonally polarized lower energy daughter photons inside a crystal with a $\chi^{(2)}$ nonlinearity. Initially, the photon pairs are entangled in energy, time, and momentum due to the energy and momentum conservation conditions that govern the process. In addition, polarization entanglement may be obtained as a result of specific local operations on the photon pair [7, 8, 9, 10]. An optical process such as this has the advantage that the photons, once generated, interact rather weakly with the environment, thus making it possible to maintain entanglement for relatively long periods of time.

In this paper, we propose and analyze efficient generation schemes for pulsed two-photon polarization entangled states. Through temporal or spectral engineering of the two-photon state produced in the type-II SPDC process pumped by a ultrafast laser pulse (ultrafast type-II SPDC), it is possible to generate pulsed polarization entangled states that are free of any post-selection assumptions. Pulsed polarization entangled states are an essential ingredient in many experiments in quantum optics. They are useful, for example, as building blocks for entangled states of three or more photons [11]. (In general, the SPDC process only results in two-photon entanglement.) Pulsed two-photon entangled states are also useful in practical quantum cryptography systems, since the well-known arrival times permit gated detection.

We begin in section II with a discussion of the limitations of the state-of-the-art techniques for the generation of polarization-entangled photon pairs. In section III, we present a universal Bell-state synthesizer, which makes use of a novel interferometric method to temporally engineer the two-photon wavefunction. We follow up in section IV with an analysis of the spectral properties of the two-photon wavefunction produced in ultrafast type-II SPDC. We then propose a method for the efficient generation of pulsed polarization entanglement via the spectral engineering of the two-photon wavefunction. We also discuss two two-photon polarization entangled states with novel spectral characteristics: the frequency-correlated state; and the frequency-uncorrelated state. Entangled states with such spectral properties might be useful for quantum-enhanced positioning and in multi-source interference experiments.

II. TWO-PHOTON ENTANGLEMENT IN ULTRAFAST TYPE-II SPDC

Let us briefly review one of the standard techniques for generating polarization entangled two-photon state via

---

*Electronic address: kimy@ornl.gov

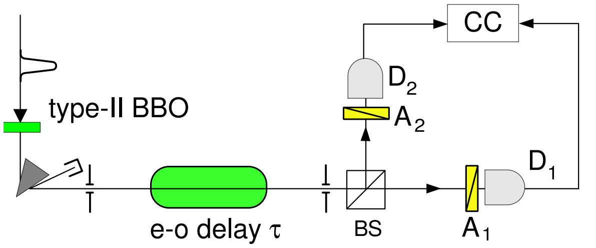

FIG. 1: Typical experimental setup for preparing a Bell-state using collinear type-II SPDC. Here, two out of four possible biphoton amplitudes are post-selected by the coincidence circuit, see Ref. [8, 9]. One can also utilize noncollinear type-II SPDC in which the amplitude post-selection assumption is not necessary, see Ref. [10].

type-II SPDC [8, 9, 10]. A typical experimental setup is shown in Fig. 1. A type-II nonlinear crystal is pumped with a UV laser beam and the orthogonally polarized signal and idler photons, which are in the near infrared, travel collinearly with the pump. After passing through a prism sequence to remove the pump, the signal-idler photon pair is passed through a quartz delay circuit (e-o delay τ) before the beamsplitter (BS) splits the SPDC beam into two spatial modes. A polarization analyzer and a single-photon detector are placed at each output port of the beamsplitter for polarization correlation measurements. In this case, the two quantum mechanical amplitudes in which both photons end up at the same detector are not registered since only coincidence events are considered. That is, a state post-selection has been made [8, 9, 12]. A noncollinear type-II SPDC method developed later resolved this state post-selection problem and is usually regarded as the "standard" method for generating polarization entangled photon pairs [10].

Both the collinear and noncollinear type-II SPDC methods work very well for the generation of polarization entangled photon pairs when the UV pump laser is continuous wave (cw). In this case, however, there is no information available regarding the photons' arrival times at the detectors. Such timing information can be quite useful in certain applications, as discussed in section I. If the UV pump has the form of an ultrafast optical pulse ($\approx$ 100 fsec), then the photon pair arrival times can be known within a time interval on the order of the pump pulse duration. However, it has been theoretically and experimentally shown that, in general, type-II SPDC suffers the loss of quantum interference if the pump is delivered in the form of an ultrafast pulse [13, 14].

We will first briefly review the theoretical treatment of the ultrafast type-II SPDC process and discuss the physical mechanism of the loss of quantum interference (or decoherence). With this understanding in hand, we then discuss in the subsequent sections two methods for eliminating this decoherence through spectral and temporal engineering of the two-photon state.

From first-order perturbation theory, the quantum state of type-II SPDC may be expressed as [9, 13]

$$|\psi\rangle = -\frac{i}{\hbar}\int_{-\infty}^{\infty} dt\, \mathcal{H}|0\rangle, \tag{1}$$

where

$$\mathcal{H} = \epsilon_0 \int d^3\vec{r}\,\chi^{(2)} E_p(z,t) E_o^{(-)} E_e^{(-)}$$

is the Hamiltonian governing the SPDC process. The pump electric field, $E_p(z,t)$, is considered classical and is assumed to have a Gaussian shape in the direction of propagation. The operator $E_o^{(-)}$ ($E_e^{(-)}$) is the negative frequency part of the quantized electric field of o-polarized (e-polarized) photon inside the crystal. Integrating over the length of the crystal, L, Eq. (1) can be written as

$$|\psi\rangle = C \iint d\omega_e d\omega_o \,\mathrm{sinc}\left(\frac{\Delta L}{2}\right) \mathcal{E}_p(\omega_e+\omega_o) a_e^\dagger(\omega_e) a_o^\dagger(\omega_o)|0\rangle, \tag{2}$$

where C is a constant and $\Delta \equiv k_p(\omega_p) - k_o(\omega_o) - k_e(\omega_e)$. The pump pulse is described by $\mathcal{E}_p(\omega_e+\omega_o) = \exp\{-(\omega_e+\omega_o-\Omega_p)^2/\sigma_p^2\}$, where σ_p and Ω_p are the bandwidth and the central frequency of the pump pulse, respectively.

For the experimental set-up shown in Fig. 1, the electric field operators at the detectors are

$$\begin{aligned} E_1^{(+)} &= \frac{1}{\sqrt{2}}\int d\omega' \,\{\cos\theta_1\, e^{-i\omega'(t_1+\tau)} a_e(\omega') - \sin\theta_1\, e^{-i\omega' t_1} a_o(\omega')\}, \\ E_2^{(+)} &= \frac{i}{\sqrt{2}}\int d\omega' \,\{\cos\theta_2\, e^{-i\omega'(t_2+\tau)} a_e(\omega') + \sin\theta_2\, e^{-i\omega' t_2} a_o(\omega')\}, \end{aligned}$$

where θ_1 and θ_2 are the angles of the polarization analyzers A_1 and A_2 and τ is the e-o delay. Here we have assumed no spectral filtering before detection. The coincidence count rate at the detectors is proportional to

$$\begin{aligned} R_c &\propto \int dt_1 \int dt_2\, |\langle 0|E_2^{(+)}E_1^{(+)}|\psi\rangle|^2 \\ &= \int dt_+ \int dt_-\, |\mathcal{A}(t_+,t_-)|^2, \end{aligned} \tag{3}$$

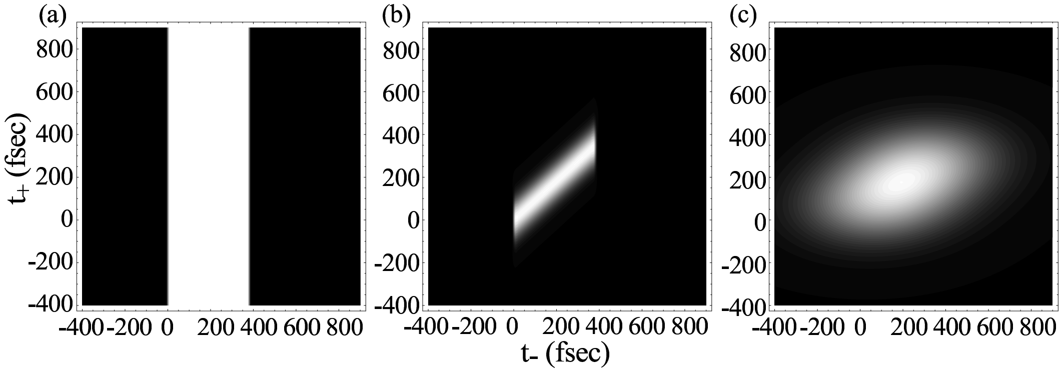

FIG. 2: Calculated two-photon wavefunction $\Pi(t_+, t_-)$ for type-II SPDC. (a) For a cw-pumped case. The two-photon wavefunction is independent of t_+ and has the rectangular shape in t_-. (b) For a 100 fsec pump pulse. It is strongly asymmetric. (c) With 5 nm bandwidth spectral filters. The two-photon wavefunction is expanded.

where $t_+ = (t_1 + t_2)/2$ and $t_- = t_1 - t_2$.

The two-photon amplitude $\mathcal{A}(t_+, t_-)$ has the form

$$\mathcal{A}(t_+, t_-) = \cos\theta_1 \sin\theta_2 \Pi(t_+, t_- + \tau) - \sin\theta_1 \cos\theta_2 \Pi(t_+, -t_- + \tau), \tag{4}$$

where

$$\Pi(t_+, t_-) = \begin{cases} e^{-i\Omega_p t_+} e^{-\sigma_p^2 \{t_+ - [D_+/D] t_-\}^2} & \text{for } 0 < t_- < DL \\ 0 & \text{otherwise.} \end{cases} \tag{5}$$

The parameters D_+ and D are defined to be

$$\begin{aligned} D_+ &= \frac{1}{2}\left(\frac{1}{u_o(\Omega_o)} + \frac{1}{u_e(\Omega_e)}\right) - \frac{1}{u_p(\Omega_p)}, \\ D &= \frac{1}{u_o(\Omega_o)} - \frac{1}{u_e(\Omega_e)}, \end{aligned}$$

where, for example, $u_o(\Omega_o)$ is the group velocity of o-polarized photon of frequency Ω_o in the crystal.

It is clear from Eqs. (3) and (4) that the degree of quantum interference is directly related to the amount of overlap between the two two-photon wavefunctions $\Pi(t_+, t_- + \tau)$ and $\Pi(t_+, -t_- + \tau)$. Figure 2 shows calculated two-photon wavefunctions for type-II SPDC in a 2 mm Beta-Barium Borate (BBO) crystal with a central pump wavelength of 400 nm. The two-photon wavefunction for the cw-pumped case is symmetric in t_+ and t_-. As shown in Fig. 2(a), it has a rectangular shape in the t_- direction and extends to infinity in the t_+ direction. In the case of ultrafast type-II SPDC, the two-photon wavefunction is strongly asymmetric, see Fig. 2(b). As we shall show shortly, this is the origin of loss of quantum interference in ultrafast type-II SPDC.

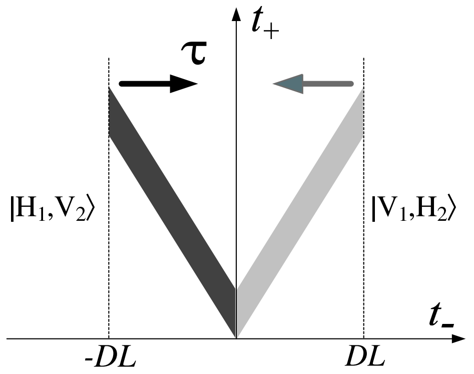

FIG. 3: Distribution of two-photon amplitude $\mathcal{A}(t_+, t_-)$ for Eq. (4). Due to little overlap between $\Pi(t_+, t_- + \tau)$ and $\Pi(t_+, -t_- + \tau)$, quantum interference visibility cannot be high. In the cw-pumped case, however, 100% quantum interference should occur, see Fig. 2(a), if τ is correctly chosen.

Having learned the exact shape of the two-photon wavefunction $\Pi(t_+, t_-)$, we are now in a position to study the overlap of the wavefunctions in Eq. (4). The situation is well illustrated in Fig. 3. When $\tau = 0$, there is no overlap at all and hence no quantum interference. Increasing τ brings the two two-photon wavefunctions together and they begin to overlap. This increases the indistinguishability of the two wavefunctions, which represent the two-photon polarization states $|V_1, H_2\rangle$ and $|H_1, V_2\rangle$. Because the two wavefunctions are symmetric in cw-pumped type-II SPDC, perfect overlap may be achieved with the proper value of τ, see Fig. 2(a). With

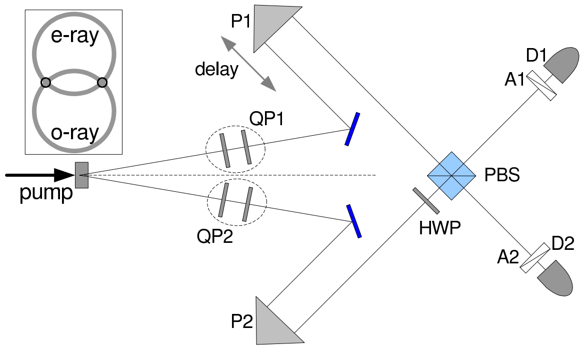

FIG. 4: Universal Bell-state synthesizer. Non-collinear type-II SPDC is used to prepare an initial polarization state which is in a mixed state. QP1 and QP2 are thin quartz plates with optic axes oriented vertically and HWP is the $\lambda/2$ plate oriented at 45°.

an ultrafast pump, however, the wavefunctions are asymmetric and perfect overlap is not possible. The amount of relative overlap may be increased in one of two ways: (i) by decreasing the thickness of the crystal; or (ii) through the use of narrowband spectral filters to expand the two-photon wavefunction, see Fig. 2(c). Both methods increase the relative amount of overlap, which in turn increase the overall indistinguishability of the system. The drawback of these methods, obviously, is the reduced number of available entangled photon pairs.

III. TEMPORAL ENGINEERING OF THE TWO-PHOTON STATE

In this section, we present a method in which complete overlap of two two-photon wavefunctions may be achieved with no change in the spectral properties of the photons. Consider the experimental setup shown in Fig. 4. A type-II BBO crystal is pumped either by a cw- or by a pulsed- pump laser. As in Ref. [10], we restrict our attention to the photons found in the intersections of the cones made by the e- and o-rays exiting the crystal [15]. A $\lambda/2$ plate rotates the polarization in one arm before the two photons are brought together at a polarizing beam splitter (PBS). Note that since the two photons always have the same polarizations when they reach the PBS, they always exit different ports. Thus, the state post-selection assumption is not necessary.

The two Feynman alternatives (reflected-reflected and transmitted-transmitted) leading to coincidence detection are shown in Fig. 5. Note that there are only two two-photon amplitudes and in both cases the e-ray (o-ray) of the crystal is always detected by D_1 (D_2). This means that, unlike the experiment discussed in the previous section, any spectral or temporal differences between the o- and e-photons provides no information at the detectors that might make it possible to distinguish between the two wavefunctions. The two biphoton wavefunctions, which represent $|H_1\rangle|H_2\rangle$ and $|V_1\rangle|V_2\rangle$, are therefore quantum mechanically indistinguishable so that the state exiting the PBS is

$$|\Phi\rangle = \frac{1}{\sqrt{2}}\left(|H_1\rangle|H_2\rangle + e^{i\varphi}|V_1\rangle|V_2\rangle\right),$$

where φ is the phase between the two terms. This phase may be adjusted by tilting the quartz plates QP1 and QP2. By setting $\varphi = 0$, the Bell state

$$|\Phi^{(+)}\rangle = \frac{1}{\sqrt{2}}\left(|H_1\rangle|H_2\rangle + |V_1\rangle|V_2\rangle\right)$$

is attained. From this state, only simple linear operations are needed to transform to any of the other Bell states.

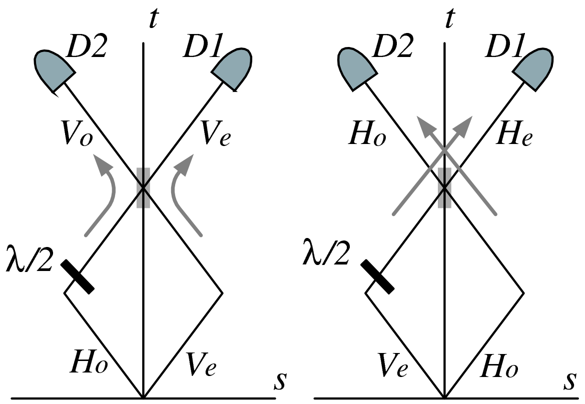

FIG. 5: Feynman alternatives for the experimental setup shown in Fig. 4. Note that e-ray (o-ray) of the crystal is always detected by D_1 (D_2) and there are only two two-photon alternatives (reflected-reflected and transmitted-transmitted). If the path length difference between the two arms of the interferometer is zero, the two alternatives (r-r and t-t) are indistinguishable in time regardless of the choice of the pump source, crystal thickness, and spectral filtering.

Let us now analyze this interferometer more formally. If we assume that the phase difference between the two amplitudes φ is set to zero, then the electric field operators that reach the detectors may be written as

$$\begin{aligned} E_1^{(+)} &= \int d\omega' \,\{\cos\theta_1\, e^{-i\omega'(t_1+\tau)} a_{Ve}(\omega') - \sin\theta_1\, e^{-i\omega' t_1} a_{He}(\omega')\}, \\ E_2^{(+)} &= \int d\omega' \,\{\cos\theta_2\, e^{-i\omega' t_2} a_{Vo}(\omega') - \sin\theta_2\, e^{-i\omega'(t_2+\tau)} a_{Ho}(\omega')\}, \end{aligned}$$

where, for example, $a_{Vo}(\omega')$ is the annihilation operator for a photon of frequency ω' with vertical polarization which was originally created as the o-ray of the crystal.

Then the two-photon amplitude $\mathcal{A}(t_+, t_-)$ may be expressed as

$$\mathcal{A}(t_+, t_-) = \cos\theta_1 \cos\theta_2 \Pi(t_+ + \tau/2, t_- + \tau) + \sin\theta_1 \sin\theta_2 \Pi(t_+ + \tau/2, t_- - \tau). \quad (6)$$

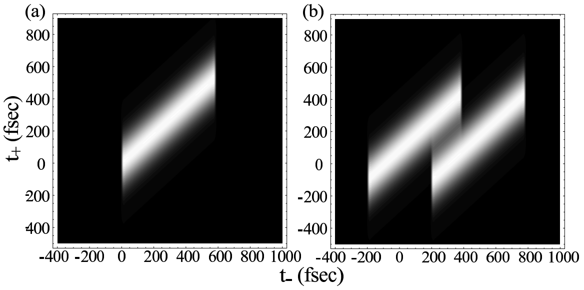

FIG. 6: Temporal engineered two-photon amplitude. This figure shows how the two two-photon wavefunctions behave as τ is introduced. (a) Two two-photon wavefunctions overlap completely when $\tau = 0$ (compare it with Fig. 3). (b) When $\tau = 200$ fsec, there is almost no overlap.

In contrast to the amplitude represented by Eq. (4), the two-photon wavefunctions on the right-hand side of Eq. (6) overlap completely when $\tau = 0$, regardless of their shape, see Fig. 6. Since complete overlap is possible for any shape of the two-photon wavefunction, this method should work for both cw-pumped and pulse-pumped SPDC. As such, this interferometer may be considered as a universal Bell-state synthesizer − perfect quantum interference may be observed regardless of pump bandwidth, crystal thickness, or SPDC wavelength, with no need for spectral filters.

The typical peak-dip effect may be observed by varying the delay τ, i.e.,

$$R_c = \begin{cases} \frac{1}{2} + \frac{1}{2}\exp(-D_+^2\sigma_p^2\tau^2/2D^2) & \text{for } \theta_1 = \theta_2 = 45^\circ \\ \frac{1}{2} - \frac{1}{2}\exp(-D_+^2\sigma_p^2\tau^2/2D^2) & \text{for } \theta_1 = -\theta_2 = 45^\circ. \end{cases}$$

Note that the thickness of the crystal L does not appear in the above equation and all other experimental parameters, D_+, σ_p, and D, only affect the width of the quantum interference, not the maximum visibility. Figure 7 shows the calculated coincidence rate as a function of the delay τ. It is easy to see that the coincidence rate R_c is a monotonically varying function of τ, with complete quantum interference expected at $\tau = 0$. This insensitivity to small changes in path length difference provides for a stable source of high-quality Bell-states. This robustness is not found in two-crystal or double-pulse pump type-II SPDC schemes, where a small phase change in the interferometer results in sinusoidal modulations at the pump central wavelength. Such schemes require active phase stabilization and, therefore, are not practical [16]. Our scheme does not suffer this disadvantage.

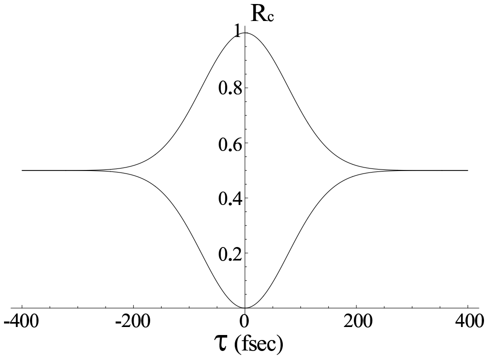

FIG. 7: Calculated space-time interference pattern as a function of delay τ in fsec. Upper line is for $\theta_1 = \theta_2 = 45^\circ$ and lower line is for $\theta_1 = -\theta_2 = 45^\circ$. The calculation is done for a 3 mm thick type-II BBO crystal pumped by a 400 nm pump pulse with bandwidth approximately 2 nm.

In addition, if $\tau \neq 0$, the amplitudes do not overlap completely and a more general state is generated:

$$\rho = \varepsilon\rho_{ent} + (1 - \varepsilon)\rho_{mix},$$

where $\rho_{ent} = |\Phi^{(+)}\rangle\langle\Phi^{(+)}|$ and $0 \leq \varepsilon \leq 1$. Such partially entangled states are called Werner states and have recently been the subject of experimental studies in the cw domain [17]. Our scheme provides an efficient way to access a broad range of two-qubit states in both the pulsed and cw domains.

IV. SPECTRAL ENGINEERING OF THE TWO-PHOTON STATE

Using the temporal engineering technique discussed in the preceding section, it is possible to generate polarization entangled states with either cw or pulsed pumping schemes. It should be pointed out that neither the asymmetry of the two-photon wavefunction nor the spectral properties of the photon pairs are affected by this technique. In this section, we are interested in removing the asymmetry shown in Fig. 2(b) through a careful choice of wavelengths of photons involved in the interaction. In this way, it is possible to obtain pulsed polarization-entangled photon pairs directly.

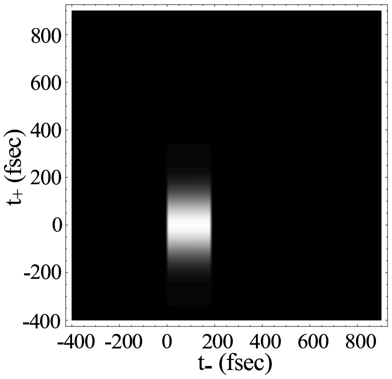

FIG. 8: Spectrally engineered two-photon wavefunction. Note that the asymmetry shown in Fig. 2(b) has disappeared. See text for details.

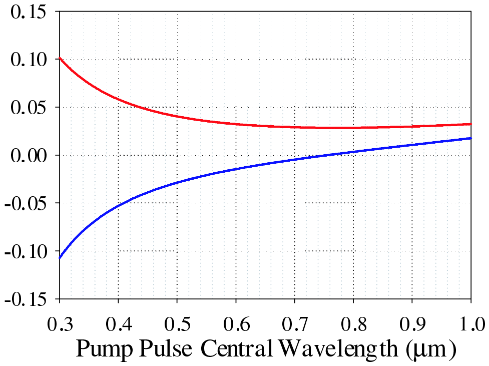

FIG. 9: D_+ (lower) and D (upper), shown in units of $1/c$, for a type-II BBO crystal. Note that $D_+ = 0$ at the pump wavelength of 757 nm. The two-photon wavefunction is symmetrized at this wavelength, see Fig. 8.

Recall that the source of poor wavefunction overlap in ultrafast type-II SPDC is the asymmetry introduced by a coupling between t_+ and t_- in the two-photon wavefunction given in Eq. (5). The approach here is to remove the coupling term so that the two-photon wavefunction becomes symmetric, as originally proposed by Keller and Rubin [13]. An example of such a wavefunction is shown in Fig. 8. Note that it has a rectangular shape in t_- (just as in cw-pumped type-II SPDC) and has a Gaussian shape in t_+ due to the Gaussian pulse envelope. It is not difficult to see that two-photon wavefunctions of this type may be completely overlapped, thus yielding full quantum interference. Therefore, pulsed polarization-entangled photon pairs may be generated using the well-known techniques described in Ref. [8, 10]. It is also expected that a triangular shaped correlation function, which has been observed in cw-pumping SPDC, should be observed in ultrafast type-II SPDC, as well.

Referring to Eq. (5), it is clear that if D_+/D is made to vanish, then $\Pi(t_+, t_-)$ becomes symmetric. Figure 9 shows the value of D_+ and D for a type-II BBO crystal as a function of pump pulse central wavelength. Note that $D_+ = 0$ when the central wavelength of the pump pulse is 757 nm. The two-photon wavefunction for this case is shown in Fig. 8 for a crystal thickness of 2 mm and a pump bandwidth of 8 nm.

In this example, this approach has an additional advantage: the entangled photon pairs are emitted with central wavelengths of 1514 nm, which is within the standard fiber communication band. Such pulsed entangled photons at communication wavelengths may be useful for building practical quantum key distribution systems using commercially installed optical fibers. At this wavelength, of course, single photon detection is more problematic. However, the recent development of single photon counting techniques using InGaAs avalanche photodiodes may soon provide good single photon counters at this wavelength [19].

We have shown that by making the D_+ term vanish through a careful choice of the pump wavelength, an initially asymmetric two-photon wavefunction can be made symmetric. Since the temporal and spectral properties of the photons are related by simple Fourier Transforms, it should come as no surprise that $D_+ = 0$ leads to a spectrally symmetric state, as well.

The spectral properties of the two-photon state from ultrafast type-II SPDC are best illustrated in plots of the two-photon joint spectrum, which can be regarded as a probability distribution for the photon frequencies. Recall that the two-photon state $|\psi\rangle$ given in Eq. (2) contains the phase mismatch term $\mathrm{sinc}(\Delta L/2)$ and the pump envelope term $\mathcal{E}_p(\omega_e + \omega_o)$. The joint spectrum function is simply the square modulus of the product of these two terms:

$$S(\omega_e, \omega_o) = |\mathrm{sinc}(\Delta L/2)\mathcal{E}_p(\omega_e + \omega_o)|^2.$$

The joint spectrum function for a typical ultrafast type-II SPDC configuration (type-II BBO pumped with an ultrafast UV pulse) is shown in Fig. 10(a). Here we have assumed $L = 2$ mm, the pump wavelength is 400 nm, the pump bandwidth is 2 nm, and the SPDC wavelength is 800 nm. Note that the joint spectrum function is asymmetric: the frequency range of the idler photon is much larger than that of the signal. The joint spectrum becomes symmetric, however, when $D_+ = 0$, as shown in Fig. 10(b). Note that the signal and the idler photons have identical spectra. Thus, the photon pair is distinguishable only in the polarizations of the photons, as required for a polarization entangled state.

The spectral properties of the photon pairs represented in Fig. 10(b) display the tendency of frequency-anticorrelation in the sense that a positive detuning for one photon is accompanied by a negative detuning for the other. This effect follows from the energy conservation condition that constrains the SPDC process. In ultrafast type-II SPDC, the anticorrelation is not as strong as in the cw-pumped case due to the broad bandwidth of the pump pulse. However, the general tendency of anticorrelation, $\omega_s = \omega_p/2 \pm \omega$ and $\omega_i = \omega_p/2 \mp \omega$ where ω is the detuning frequency, is clearly visible in Fig. 10.

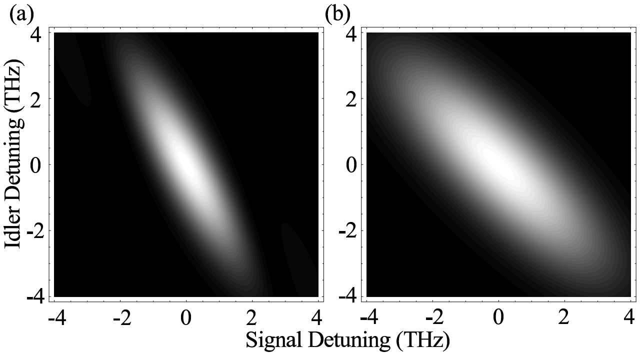

FIG. 10: Calculated joint spectrum showing frequency-anticorrelation between the signal and the idler photons. (a) Typical frequency-anticorrelated state with asymmetric joint spectrum. Pump central wavelength is 400 nm. (b) The asymmetry has now disappeared. The pump central wavelength is 757 nm and the bandwidth is 8 nm.

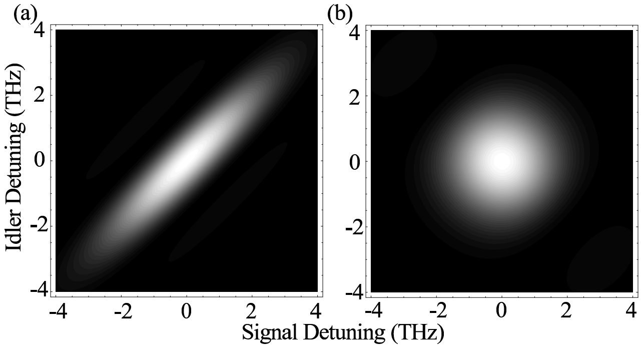

FIG. 11: (a) Calculated joint spectrum showing frequency-correlated two-photon state. The pump bandwidth is 20 nm and the crystal is 12 mm thick type II BBO. (b) Frequency-uncorrelated state. The pump bandwidth is 10 nm and the crystal is 5 mm thick type-II BBO. The pump central wavelength is 757 nm for both cases to ensure $D_+ = 0$ is satisfied.

This frequency-anticorrelation, however, is not a required feature of the two-photon state. In ultrafast type-II SPDC, two-photon states with novel spectral characteristics – the frequency-correlated state and the frequency-uncorrelated state – may be generated through appropriate choices of the parameters that affect the joint spectrum.

The idea behind two-photon states with novel spectral characteristics is not new. The output characteristics of a beamsplitter and a Mach-Zehnder interferometer for frequency-correlated and frequency-uncorrelated photon pairs are theoretically studied in Ref. [20] with no discussion of how such states might be generated. Frequency-correlated states are also studied in Ref. [21], but the discussions are limited to the generation of frequency-correlated states using quasi-phase matching in a periodically poled crystal. Here, we discuss how frequency-correlated states and frequency-uncorrelated states may be generated via appropriate spectral engineering of the two-photon state in ordinary bulk crystals. Since our main focus is polarization entangled photon pairs with novel spectral characteristics, we restrict our attention to the case in which the two-photon joint spectrum is symmetric, i.e., $D_+ = 0$.

Frequency-correlated state generation via the SPDC process is somewhat counter-intuitive since conservation of energy requires the frequencies of the photon pair to sum to the frequency of the pump photon. This requirement imposes a strong constraint in cw-pumped SPDC, where the pump the pump field is monochromatic. In ultrafast SPDC, however, the pump field has a bandwidth of several terahertz frequency (several nanometers in wavelength) and so the frequencies of the photon pair need only sum to some value within the range of pump frequencies. This extra freedom makes it possible to generate the frequency-correlated state.

Examination of the joint spectrum function $S(\omega_s, \omega_i)$ suggests that if the bandwidth of the pump envelope $\mathcal{E}_p(\omega_s + \omega_i)$ is large enough and if the parameters are chosen such that the $\sin(\Delta L/2)$ may be approximated by the delta function $\delta(\omega_s - \omega_i)$, then the two-photon state becomes

$$|\psi\rangle = C \int d\omega \, \mathcal{E}_p(2\omega) a_s^\dagger(\omega) a_i^\dagger(\omega) |0\rangle, \qquad (7)$$

where C is a constant. Eq. (7) shows the signature of the frequency-correlated state: $\omega_s = \omega_p/2 \pm \omega$ and $\omega_i = \omega_p/2 \pm \omega$. Figure 11(a) shows the calculated joint spectrum function for the frequency-correlated two-photon state. In this example, the pump central wavelength was set to 757 nm in order to satisfy the condition $D_+ = 0$, i.e., to assure direct generation of polarization entangled photon pairs. This also has the effect of properly aligning the $\mathrm{sinc}(\Delta L/2)$ function. The only other requirement is that this function should be narrow enough that it may be approximated as $\delta(\omega_s - \omega_i)$. This is achieved by increasing the value of L, the crystal thickness, since the width of the sinc function is inversely proportional to the crystal length. In Fig. 11(a), it is assumed that a 12 mm thick type-II BBO crystal is pumped by a 20 nm bandwidth ultrafast pulse centered at 757 nm and that, at zero detuning, the wavelengths of the SPDC photons are 1514 nm. The structure of frequency-correlation is clearly illustrated: as the signal detuning increases, the idler detuning is also increased. Such frequency-correlated states have been shown to be useful for certain quantum metrology applications [5].

By slightly modifying the condition for the generation of the frequency-correlated state, it is possible to generate the frequency-uncorrelated state. By frequency-uncorrelated state, we mean that the frequencies of the two photons are uncorrelated, in the sense that the range of the available frequencies for a particular photon is completely independent of the frequency of its conjugate. As far as the photons are concerned, this means that the spectral properties of one photon are in no way correlated with the spectral properties of the other. The joint spectrum of such a state is shown in Fig. 11(b) where the joint spectrum function is calculated for type-II SPDC in a 5-mm thick BBO crystal pumped by a 10 nm bandwidth ultrafast pump centered at 757 nm. Again, the pump pulse central wavelength is set to 757 nm to ensure symmetry in the joint spectrum. The more general case is discussed in Ref. [18], where it is also shown that such states are essential in experiments involving interference between photons from different SPDC sources.

V. SUMMARY

The generation of polarization entangled states requires the coherent superposition of two two-photon wavefunctions. An additional requirement is that the two wavefunctions must be identical in all respects except polarization. This is not the case, in general, when the photon pairs originate in a type-II SPDC process, although only a simple delay is required when the process is pumped by a cw laser. When an ultrafast pumping scheme is employed, however, these techniques typically do not result in the complete restoration of quantum interference. Some improvement is seen with (i) thin nonlinear crystals and/or (ii) narrow spectral filters before the detectors. Unfortunately, both of these techniques result in greatly reduced count rates. By engineering the two-photon state of ultrafast type-II SPDC in time or in frequency, it is possible to recover the quantum interference without discarding any photon pairs. In addition, spectral engineering holds the promise of two-photon states with novel spectral properties which have not been available previously.

The temporal engineering of the two-photon state is accomplished through a novel interferometric technique which changes the temporal distribution of the two-photon amplitude $\mathcal{A}(t_+, t_-)$, which is comprised of two two-photon wavefunctions $\Pi(t_+, t_-)$. The shapes of the wavefunctions are not altered in this process – only the way in which they overlap in $\mathcal{A}(t_+, t_-)$. The temporally engineered source does not suffer the loss of quantum interference common in ultrafast type-II SPDC and the interferometer can be viewed as a universal Bell-state synthesizer since the quantum interference is independent of the crystal properties, the bandwidth of spectral filters, the bandwidth of the pump laser, and the wavelengths.

A different approach is taken in the spectral engineering technique. Here, the asymmetric two-photon wavefunction $\Pi(t_+, t_-)$ from ultrafast type-II SPDC is symmetrized through careful control of the crystal and pump properties. Such spectrally engineered two-photon states exhibit complete quantum interference with no need for auxiliary interferometric techniques. The spectral engineering techniques may also be employed in the generation of two-photon states with novel spectral characteristics: the frequency-correlated state and the frequency-uncorrelated state. Unlike typical two-photon states from the SPDC process, which exhibit strong frequency-anticorrelation, the frequency-correlated state is characterized by a strong positive frequency correlation, while the frequencies of the two photons are completely uncorrelated in the frequency-uncorrelated state.

The temporal and spectral engineering techniques studied in this paper are expected play an important role in generating the pulsed entangled photon pairs essential in applications such as practical quantum cryptography, multi-photon entangled state generation, multi-photon interference experiments, etc. Since temporal engineering allows one to control the decoherence in a stable way, it also facilitates the study of the effects of decoherence in entangled multi-qubit systems. In addition, frequency-correlated discussed in this paper may be useful for certain quantum metrology applications.

Acknowledgments

We would like to thank M.V. Chekhova, S.P. Kulik, M.H. Rubin, and Y. Shih for helpful discussions. This research was supported in part by the U.S. Department of Energy, Office of Basic Energy Sciences. The Oak Ridge National Laboratory is managed for the U.S. DOE by UT-Battelle, LLC, under contract No. DE-AC05-00OR22725.

[1] A. Einstein, B. Podolsky, and N. Rosen, Phys. Rev. **47**, 777 (1935); J.S. Bell, Speakable and unspeakable in quantum mechanics, Cambridge University Press, New York (1987).

[2] A. Steane, Rep. Prog. Phys. **61**, 117 (1998); M.A. Nielson and I.L. Chuang, Quantum Computation and Quantum Information, Cambridge University Press, New York (2000).

[3] A.N. Boto *et al.*, Phys. Rev. Lett. **85**, 2733 (2000); M. D'Angelo, M.V. Chekhova, and Y. Shih, Phys. Rev. Lett. **87**, 013602 (2001);

[4] J.P. Dowling, Phys. Rev. A **57**, 4736 (1998).

[5] R. Jozsa *et al.*, Phys. Rev. Lett. **85**, 2010 (2000); V. Giovannetti, S. Lloyd, and L. Maccone, Phys. Rev. A **65**, 022309 (2002).

[6] D.N. Klyshko, Photons and Nonlinear Optics, Gordon and Breach, New York (1988).

[7] T.E. Kiess *et al.*, Phys. Rev. Lett. **71**, 3893 (1993).

[8] Y.H. Shih and A.V. Sergienko, Phys. Lett. A **186**, 29 (1994); Y.H. Shih and A.V. Sergienko, Phys. Lett. A **191**, 201 (1994)

[9] M.H. Rubin *et al.*, Phys. Rev. A **50**, 5122 (1994).

[10] P.G. Kwiat *et al.*, Phys. Rev. Lett. **75**, 4337 (1995).

[11] T.E. Keller *et al.*, Phys. Rev. A **57**, 2076 (1998).

[12] L. De Caro and A. Garuccio, Phys. Rev. A **50**, R2803 (1994); S. Popescu, L. Hardy, and M. Zukowski, Phys. Rev. A **56**, R4353 (1997); M. Zukowski *et al.*, Phys. Rev. A **60**, R2614 (1999).

[13] T.E. Keller and M.H. Rubin, Phys. Rev. A **56**, 1534 (1997); W.P. Grice and I.A. Walmsley, Phys. Rev. A **56**, 1627 (1997).

[14] G. Di Giuseppe *et al.*, Phys. Rev. A 56, R21 (1997); W.P. Grice *et al.*, Phys. Rev. A **57**, R2289 (1998); Y.-H. Kim *et al.*, Phys. Rev. A **64**, 011801(R) (2001); Y.-H. Kim *et al.*, Phys. Rev. Lett. **86**, 4710 (2001).

[15] The common misconception is that the photon pairs emerging from these two cross sections are automatically polarization entangled. As we have discussed in section II, the polarization state of the photon pair is in a mixed state

$$\rho_{mix} = \frac{1}{2}\left(|H_1\rangle|V_2\rangle\langle V_2|\langle H_1| + |V_1\rangle|H_2\rangle\langle H_2|\langle V_1|\right).$$

[16] D. Branning *et al.*, Phys. Rev. Lett. **83**, 955 (1999); J.H. Shapiro and F.N.C. Wang, J. Opt. B **2**, L1 (2000); Y.-H. Kim *et al.*, Phys. Rev. A **63**, 062301 (2001); A.V. Burlakov *et al.*, *ibid.* **64**, 041803(R) (2001).

[17] R.F. Werner, Phys. Rev. A **40**, 4277 (1989); P.G. Kwiat *et al.*, Nature **409**, 1014 (2001); A.G. White *et al.*, Phys. Rev. A **65**, 012301 (2001).

[18] W.P. Grice, A.B. U'Ren, and I.A. Walmsley, Phys. Rev. A **64**, 063815 (2001).

[19] A. Lacaita *et al.*, Applied Optics **35**, 2986 (1996); G. Ribordy *et al.*, Applied Optics **37**, 2272 (1998); A. Karlsson *et al.*, IEEE Circuits & Devices, Nov., 34, (1999); P.A. Hiskett *et al.*, Applied Optics **39**, 6818 (2000).

[20] R.A. Campos, B.E.A. Saleh, and M.C. Teich, Phys. Rev. A **42**, 4127 (1990).

[21] V. Giovannetti *et al.*, quant-ph/0109135.